

Research Paper

Silver Nanoparticle Exposure Induced Mitochondrial Stress, Caspase-3 Activation and Cell Death: Amelioration by Sodium Selenite

Wanrui Ma^{†1,4}, Li Jing^{†2,4}, Alexandra Valladares³, Suresh L. Mehta^{4,5}, Zhizhong Wang⁶, P. Andy Li⁴✉, John J. Bang^{3,4} ✉

1. Department of Comprehensive Medicine, General Hospital of Ningxia Medical University, Yinchuan, Ningxia, P.R. China
2. Department of Pathology, College of Basic Sciences, Ningxia Medical University, Yinchuan, Ningxia, P.R. China
3. Department of Environmental, Earth and Geospatial Sciences, North Carolina Central University, Durham, North Carolina, USA.
4. Department of Pharmaceutical Sciences, Biomanufacturing Research Institute and Technological Enterprise (BRITE), North Carolina Central University, Durham, North Carolina, USA.
5. Department of Neurological Surgery, University of Wisconsin, School of Medicine and Public Health, Madison, WI 53792, USA
6. Department of Epidemiology and Biostatistics, School of Public Health, Ningxia Medical University, Yinchuan, China

†Equal contribution

✉ Corresponding authors: Dr. John J Bang, email: jbbang@nccu.edu; or Dr. P. Andy Li, email: pli@nccu.edu

© 2015 Ivyspring International Publisher. Reproduction is permitted for personal, noncommercial use, provided that the article is in whole, unmodified, and properly cited. See <http://ivyspring.com/terms> for terms and conditions.

Received: 2015.03.06; Accepted: 2015.04.20; Published: 2015.06.01

Abstract

Silver nanoparticles (AgNP), one of the most commonly used engineered nanomaterial for biomedical and industrial applications, has shown a toxic potential to our ecosystems and humans. In this study, murine hippocampal neuronal HT22 cells were used to delineate subcellular responses and mechanisms to AgNP by assessing the response levels of caspase-3, mitochondrial oxygen consumption, reactive oxygen species (ROS), and mitochondrial membrane potential in addition to cell viability testing. Selenium, an essential trace element that has been known to carry protecting property from heavy metals, was tested for its ameliorating potential in the cells exposed to AgNP. Results showed that AgNP reduced cell viability. The toxicity was associated with mitochondrial membrane depolarization, increased accumulation of ROS, elevated mitochondrial oxygen consumption, and caspase-3 activation. Treatment with sodium selenite reduced cell death, stabilized mitochondrial membrane potential and oxygen consumption rate, and prevented accumulation of ROS and activation of caspase-3. It is concluded that AgNP induces mitochondrial stress and treatment with selenite is capable of preventing the adverse effects of AgNP on the mitochondria.

Key words: Engineered nanomaterial, Silver nanoparticles, Mitochondrial stress, Caspase, Reactive Oxygen Species, Cell death, Selenium

Introduction

With the advent of new surface treatment techniques and nanotechnology, the applications of silver particles in nano regime (also called silver nanoparticles or AgNP) have been steadily increased not only as antimicrobial and disinfecting agents but also as a treatment agent on various types of diseases [1]. As the use of silver in consumer products and biomedical

applications continues to increase, there have been exposure-induced toxicity concerns on our ecosystems and human health. Recently AgNP have been detected in our water systems such as wastewater treatment plant, which raised an issue of exposure induced health impacts on human [2,3]. In more controlled environmental conditions simulating real life

conditions, investigation also has revealed concerning level of toxicity issues in plants, insects, fish, and animals with a wide range of abnormal manifestations such as depigmentation secondary to a potentially dysfunctional dopamine pathway, delay in development, and motor neuron defect [4-6]. Studies indicated that the effects of silver are presented in several different mechanisms including its capacity of binding to DNA, influencing membrane structures and their functions, and manipulating both reactive oxygen species dependent and independent pathways, among others [7-9]. The exposure-induced toxic effects of silver also seem to be dependent on the physicochemical conditions of the exposed silver (i.e., particles vs. ionic form) and the environmental media where the silver is present [10,11]. Both apoptotic and necrotic cell death pathways are also known to be involved [12]. With increased probability of exposure to AgNP with its toxicity profile becoming more evident, both understanding the toxicological mechanisms involved and finding amelioration methods are very relevant and imminent issues in this technology-driven society.

Selenium is an essential micronutrient, which is well-known for its detoxifying effects in heavy metal exposure [13]. Selenium deficiency is associated with many diseases including endemic fatal cardiomyopathy (Keshan disease), chronic degenerative diseases [14], impaired cognitive function and neurological disorders [15]. Selenium supplementation has been suggested to have a protective role in various diseases, such as viral infection [16], immune system function [17] and neurodegenerative disease [18,19]. Studies have shown that selenium is capable of restoring the activity of important antioxidant enzymes such as glutathione peroxidases and thioredoxin reductase [20-22]. A recent study has shown that expo-

sure to AgNPs leads to the inhibition of selenoprotein synthesis and inhibition of thioredoxin reductase isoform 1 (TrxR1) enzyme [23]. Therefore, it is tempting to speculate that selenium may be an effective agent for protecting cells from AgNP exposure.

Materials and Methods

Material Characterization

Silver nanoparticles of various sizes ranging between 15nm and 100nm were purchased (Sun Nano, California). Transmission electron microscopic examination (TEM) was performed for physical characterization followed by dynamic light scattering (DLS) assessment. The size of majority of AgNP under TEM was around 30nm that was consistent with the values estimated by DLS on stock solutions prepared (Figure 1). Before TEM analysis, AgNP sample from stock suspension was sonicated for at least 30 minutes in nanopure water. The same samples were used for DLS analysis which showed 20-30 nm range at 5 ppm concentration. For DLS hydrodynamic diameter measurement, ALV-CGS3 (ALVgmbh, Langen, Germany) was used.

Cell culture and experimental treatments

Murine hippocampal HT22 cells were cultured in DMEM containing 10% fetal bovine serum (FBS), 200 mM streptomycin/penicillin (Invitrogen), and 2 mM glutamine. The cells were maintained at 90%-95% relative humidity in 5% CO₂ at 37 °C. The culture medium was renewed every 2 days. Silver nanoparticles (AgNP) of different sizes (20 - 100nm) were purchased (SunNano, CA). AgNP size of 30nm was used for its toxicity in this study by using an existing prescreening data as shown in our previous studies [4, 24].

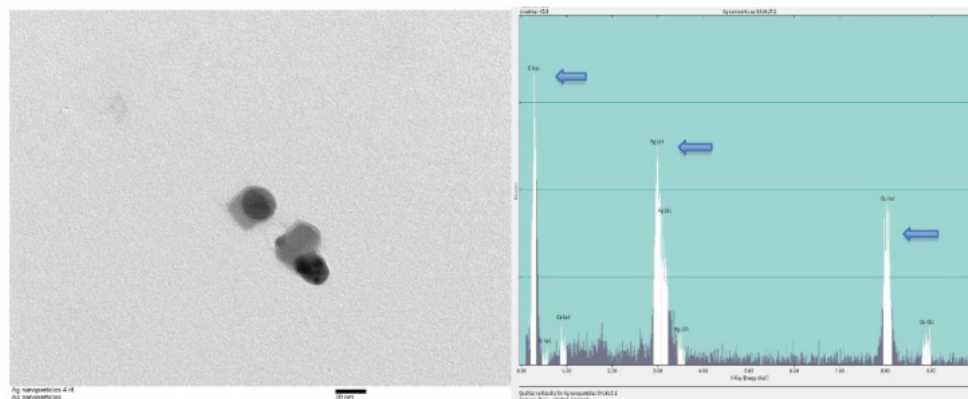


Figure 1. TEM and EDS of AgNP. (A) Stock suspension was diluted for TEM image and the sizes of the AgNP were measured between 25 and 35nm. The insert bar is 20nm long. (B) EDS indicates the presence of silver on a copper grid with formvar. Arrows from left to right indicates carbon (formvar grid support), silver (Ag NP), and copper (grid).

AgNP stock solutions with different concentrations ranging from 0.5 ppm to 5 ppm were prepared in nanopure water and stored in dark room in amber glass bottles for the study in the same way as it was prepared in our previous study [25]. For the evaluation of the effects of sodium selenite on HT22 cells exposed to various concentrations of AgNP, sodium selenite (25–200 nM) was added to the culture media 3 h prior to the cells exposed to AgNP.

Cell viability

Alamar blue assay (Thermo Fisher Scientific, Waltham, MA, USA) was used to examine cell viability. Viable cells take up the Alamar blue and the fluorescent intensity could be detected using a plate reader. HT22 cells were seeded in 96-well plates at a density of 8,000 cells per well. Various concentrations of selenium (25, 50, 100, 200 nM) were given 3 h prior to AgNP (0.5, 1.0, 1.5, 2.0, 5.0 ppm) incubation. After 24 h of AgNP exposure, the cells in each well were incubated with 10 μ l Alamar blue (1 mg/ml) at a final concentration of 100 μ g/ml for 3 h and the results were read using PHERA Star Microplate Reader (BMG Labtech, Ortenberg, Germany) at the excitation and emission wavelengths of 520 and 570 nm, respectively.

Detection of superoxide

Intracellular superoxide anion production was measured using dihydroethidine (DHE) as a fluorescent probe (Life Technologies, Grand Island, NY, USA). In brief, cells (2×10^6 /mL) were harvested and incubated with the DHE (2.5 mM) at the end of experiments for 30 min at 37 °C in a CO₂ incubator. They were then washed two times, resuspended in phosphate buffered saline (PBS). The fluorescence intensity was analyzed using Fluoromax-4 spectrofluorometer (HORIBA Jobin Yvon Inc, Edison, NJ) at the excitation and emission wavelengths of 480 nm and 590 nm, respectively. The fluorescence recorded was showed as relative fluorescent intensity (RFI).

Measurements of mitochondrial membrane potential

Mitochondrial membrane potential was measured using the tetramethyl rhodamine methyl ester (TMRM). In brief, cells (1×10^6 /mL) were incubated with TMRM (30 nM) for 30 min at 37 °C in a CO₂ incubator. Cells were washed in PBS and fluorescence was measured using a Fluoromax-4 spectrofluorometer (HORIBA Jobin Yvon Inc, Edison, NJ) at excitation and emission of 530 and 573 nm, respectively. At the end of experiments, mitochondrial potential was dissipated with carbonylcyanide p-trifluoromethoxy-

phenylhydrazone (FCCP 5 μ M), which is used as a positive control.

Immunocytochemistry

The cells were cultured in 8-well Lab-Tek II Chamber Slide system (thermoFisher Scientific Inc.). At the end of each experiment, cells were fixed within 4% paraformaldehyde for 20 min at room temperature and processed for immunocytochemistry. After permeabilization with 0.1% Triton X-100, the cells were incubated overnight at 4 °C with the monoclonal anti-cleaved caspase-3 antibody (1:200 dilution, ASP175, Cell Signaling) followed by incubation with a secondary donkey anti-rabbit Alexa Fluor 488 conjugate (Invitrogen) for 1 h at room temperature. The chambers were removed and glass slides were covered with cover slips and mounted with Vectashield Hardset Mounting Media (H-1200) containing DAPI. The results were examined using fluorescence confocal microscope (Nikon Eclipse C1). Three microscopic fields at 400X were randomly captured and the number of positively stained cells was counted.

Mitochondrial oxygen consumption measurement

Oxygen consumption was measured with high-resolution respirometry (Oxygraph, Oroboros Instruments, Innsbruck, Austria) in a glass chamber at 37°C. Each well contains 2 ml of media (DMEM with 10% FBS) and 5×10^6 cells. The medium was equilibrated by constant stirring (750 rpm) in ambient room air for 10 min. The chamber was closed to start recording the oxygen consumption at 2 seconds intervals and the recording was stopped after stabilization of the O₂ consumption signal. Respiration was finally inhibited with rotenone (0.5 mM). The oxygen consumption was calculated using DataGraph software (Oroboros Instruments). Each individual experiment was performed in two chambers in parallel, and was recorded simultaneously for paired comparisons of the oxygen consumption of each individual experiment. Respiration rates were computed and data were transformed into percent of respiration rate of control.

Statistical Analysis

All data are presented as means \pm SD. Multiple comparisons were performed with one-way ANOVA followed by Scheffe's or Tukey's tests as indicated in the figure legends. A value of $p < 0.05$ was considered statistically significant.

Results

Toxicity of AgNP on cell viability

The cell toxicity of AgNP was determined after 24 h following various amounts of nano-silver particle

incubation. The results showed that there was an inverted linear relationship between the concentration of AgNP and cell viability. As shown in **Figure 2**, at a low concentration of 0.1 ppm, AgNP did not induce cell death. When its concentration increased to 1.0 ppm, the viability decreased to 60%, and further declined to 35% and 10% when the AgNP increased to 2.0 ppm and 5.0 ppm, respectively.

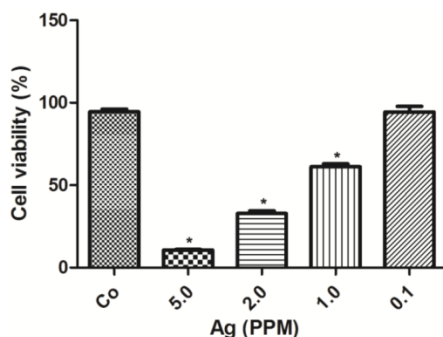


Figure 2. AgNP cell toxicity detected using alamar blue assay. The viability decreased with increased concentrations of AgNP. Data were collected from 3 or more independent experiments and presented as means \pm s.d. One-way ANOVA followed by post-hoc Scheffe's test. * $p < 0.001$ vs. control.

Selenium protection against AgNP induced cell death

The potential protective effect of selenium was examined in cells pretreated with sodium selenite for 3 h prior to AgNP incubation. As shown in **Figure 3**, selenium *per se* did not cause cell death with a concentration up to 200 nM (fill bars). Selenite pretreatment, in fact, significantly enhanced cell survival in AgNP exposed cells in a dose dependent manner. At the concentration of 25 nM, selenium increased the percentage of viable cells from 35% in AgNP (2.0 ppm) to 68%. Accordingly, the percent of viable cells increased along with the elevation of selenium and reached to 85% at a concentration of 200 nM. Because selenium at the concentration of 200 nM provided the

best protective effect, this concentration was used for rest of the experiments.

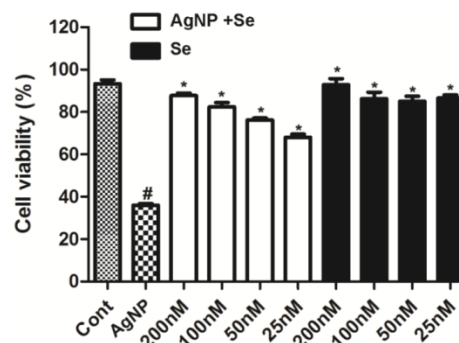


Figure 3. The protective effect of selenium against AgNP toxicity in HT22 cells. Cell viability decreased to 35% in 2.0 ppm AgNP treated cells. Pretreatment of selenium significantly increased the cell viability. Selenium *per se* did not influence the cell viability. Data were collected from at least 3 independent experiments and presented as means \pm sd. One-way ANOVA followed by post-hoc Scheffe's test. # $p < 0.01$ vs. control and * $p < 0.001$ vs. non-selenium treated AgNP exposed cells.

Selenium reduced AgNP exposure-induced ROS production

To evaluate the influence of AgNP on ROS generation, we detected superoxide levels using DHE fluorescent probe. AgNP incubation for 24 h significantly increased the superoxide level to about 30% higher than the control ($p < 0.05$). Pretreatment with 200 nM selenium brought the superoxide level down to the control level (**Fig. 4**).

Selenium prevented AgNP induced mitochondrial depolarization

Mitochondrial membrane potential was measured by TMRM fluorescent probe. AgNP incubation for 24 h moderately decreased mitochondrial membrane potential, while pretreatment with 200 nM selenium prevented the membrane potential depolarization caused by AgNP (**Fig. 5**).

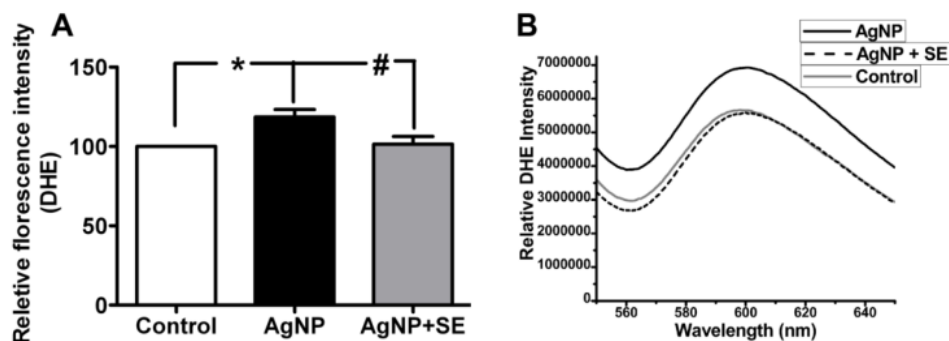


Figure 4. Detection of superoxide levels in AgNP and selenium treated cells using DHE. (A) Bar graph showing AgNP increased ROS production by close to 30% and selenium normalized the ROS level. (B) Representative original recordings. Data are collected from 3 independent experiments. Values are means \pm s.d. and analyzed by one-way ANOVA test followed by Tukey's test. * $p < 0.05$ vs. control; # $p < 0.05$ vs. AgNP.

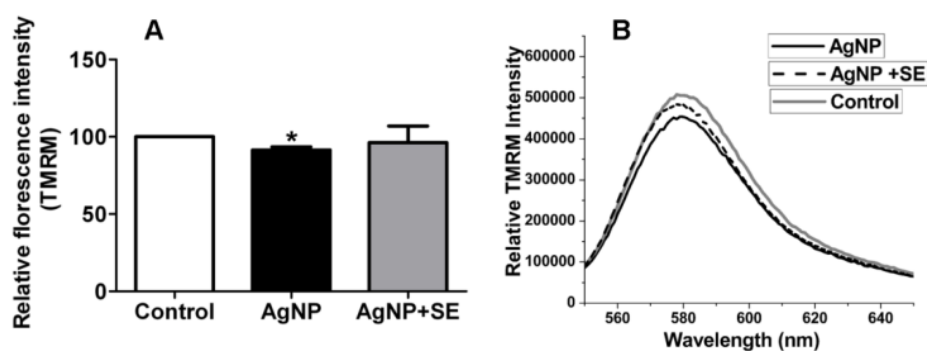


Figure 5. Mitochondrial membrane potential tested by TMRM. (A) Bar graph shows the depolarization after AgNP incubation and the preventive effect of selenium. (B) Representative original recordings. Data were collected from 3 independent experiments and presented as means \pm s.d. Data were analyzed by one-way ANOVA test followed by Tukey's test. * $p < 0.05$ vs. control.

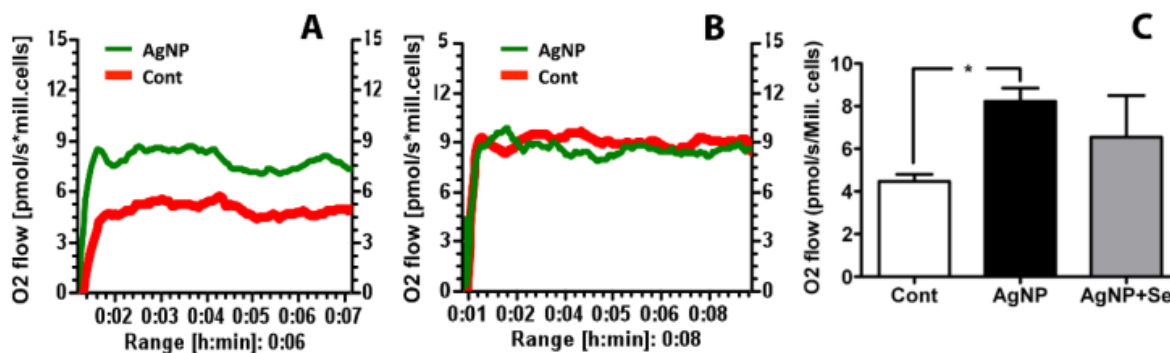


Figure 6. Mitochondrial oxygen utilization in AgNP and selenium treated cells. (A) Original recording showing increased oxygen consumption in AgNP exposed cells comparing to control cells. (B) Original recording showing selenium pretreatment inhibited the elevated oxygen consumption caused by AgNP. (C) Bar graph summarizes the average oxygen flow in 3 experimental groups. Data were collected from 3 independent experiments and presented as means \pm s.d. Data were analyzed by one-way ANOVA test followed by Tukey's test. * $p < 0.05$ vs. control.

Mitochondrial Oxygen Utilization

The mitochondrial oxygen utilization was measured to evaluate the effects of AgNP on mitochondrial function. It was found that AgNP incubation for 24 h significantly increased basal cellular respiration in HT22 cells as compared to control. Pretreatment of selenium reduced oxygen consumption to control level (Figure 6).

AgNP induced caspase-3 activation

AgNP increased active caspase-3 positive neurons while selenium suppressed such increase. In control cultures, none or occasional scattered caspase-3 positively stained neurons were observed (Figure 7A-C). After 24 h of AgNP incubation, the number of caspase-3 positive cells significantly increased to 25 per high power microscopic field (HPF) ($p < 0.001$, Figure 7D-F). Treatment with 200 nM sodium selenite reduced the positive cells down to 15/HPF (Figure 7G-I, $p < 0.05$ vs. AgNP group). Negative control cells did not show any positive caspase-3 immunostaining (Figure 7J-L). A summarized bar graph is given in Figure 7K.

Discussion

The present study explored the effect of selenium on AgNP-induced neuronal cell death. The results have demonstrated that AgNP reduces cell viability and this toxicity was associated with mitochondrial membrane depolarization, increased accumulation of ROS, elevated mitochondrial oxygen consumption, and caspase-3 activation. Treatment with sodium selenite has successfully reduced cell death, stabilized mitochondrial membrane potential and oxygen consumption rate, and prevented accumulation of ROS and activation of caspase-3.

The extent of silver nanoparticle toxicity on cells varies depending on the size of the AgNP. Those AgNP with their sizes less than 100 nm invariably showed toxicity of various extents. Among those smaller than 100 nm, AgNP about 30 nm and smaller seemed to inflict more cell damage as indicated in various studies [14]. In our study, AgNP with their size ranging between 20 and 100 nm were used for prescreening (data not shown). Those at around 30 nm size range have demonstrated the lowest cell viability across different concentration ranges (0.5- 5.0 ppm) in a concentration dependent manner. At 0.5

ppm concentration of AgNP, the cell viability was close to that of the background level (i.e. control group). The LD50 level in this study showed somewhere between 1 and 2 ppm of AgNP. Despite reaching 1-2 ppm concentration in ambient environment is less likely to happen in normal condition, it is a condition that can be easily created in occupational settings.

ROS play a critical role in triggering cell damage processes including the formation of mitochondrial permeability transition pore (MPTP) that will lead to activation of mitochondria-dependent cell death pathways [26-28]. High lipid containing organs such as the brain are vulnerable to oxidative stress [29]. In the present study, we observed superoxide radicals were increased after AgNP incubation. This finding is in agreement with the experiment conducted in human lung epithelial adenocarcinoma cells A549 [8] and rat blood serum [30]. Selenium prevented the AgNP-induced increase in ROS. These results suggest that AgNP induces oxidative stress to the cells while selenium possesses anti-oxidant effect.

Mitochondria play an important role in causing cell death by initiating cell death pathways. The mitochondrial membrane depolarization is considered to be an initial step for activation of the intrinsic cell

death pathways [31]. It is well known that increases in ROS production, and/or increased intracellular/ intra-mitochondrial calcium concentration triggers the formation of the MPTP. Depolarized mitochondrial membrane potential has been used as an indicator for the formation of MPTP [32]. In this study, we have found that AgNP induced a moderate mitochondrial membrane depolarization suggesting formation of the MPTP in AgNP incubated cells. Selenium maintained the mitochondrial membrane potential, thus prevented the formation of the MPTP. Theoretically, mitochondrial membrane potential depolarization is associated with decreased mitochondrial function as reflected by decreased oxygen consumption. Unexpectedly, we observed an increase in mitochondrial oxygen consumption after AgNP incubation. Such an increase may reflect mitochondrial response to stress in early phase. In one hand, increased oxygen improves mitochondrial function; on the other hand, increased electron flow is associated with increased chances of ROS formation. In fact, the increased ROS level in AgNP treated cells may reflect this aspect. Nevertheless selenium treatment stabilized mitochondrial oxygen consumption and reduced ROS production.

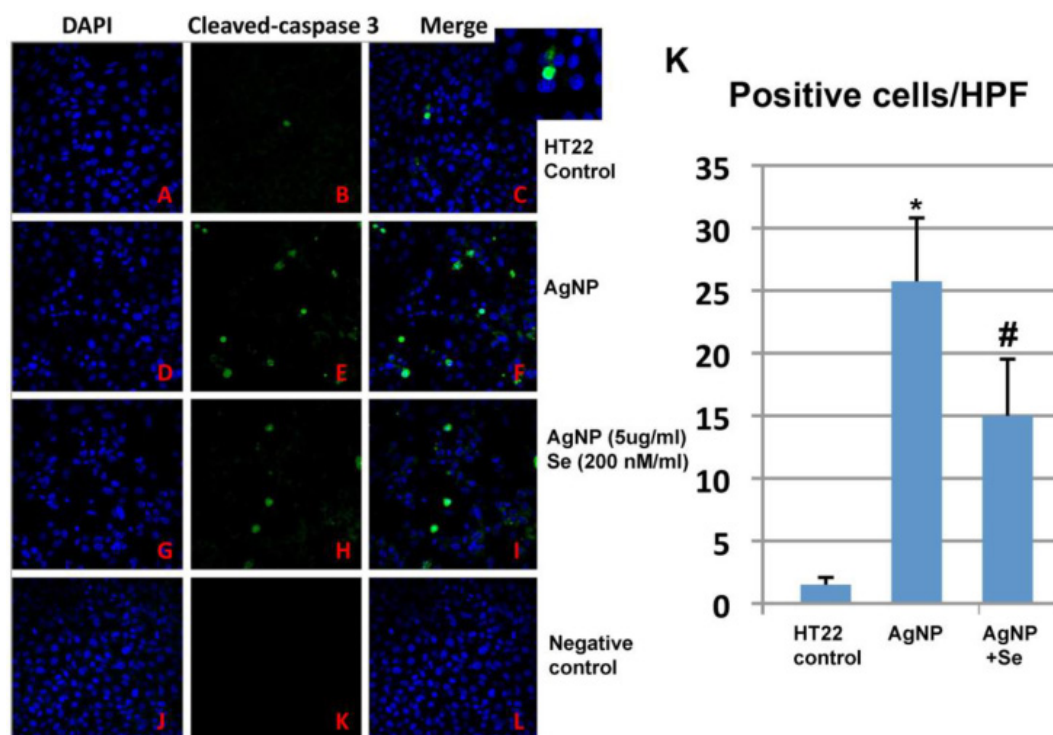


Figure 7. Caspase-3 immunocytochemistry in control, AgNP and selenium treated cells. (A-C) Control group showing occasional caspase-3 positively stained neurons. (D-F) AgNP caused increase in numbers of caspase-3 positive neurons. (G-I) Selenium decreased the number of caspase-3 positive cells. (J-L) Negative control group. (K) Summarized bar graph showing average numbers of caspase-3 positive neurons among the experimental groups. Green color denotes cleaved caspase-3 staining and blue for nuclear marker DAPI. Data were collected from 3 independent immunocytochemistry experiments, each performed in triplicate. Values are presented as means \pm s.d. HPF, high power field. * $p < 0.001$ vs. control, # $p < 0.05$ vs. AgNP.

Formation of the MPTP activates mitochondria-initiated cell death pathways, which include caspase dependent and caspase-independent pathways. The MPTP allows apoptosis-inducing factor (AIF) and endonuclease G (EndoG) to be released from the mitochondrion to nucleus. The MPTP can also cause cytochrome c and Smac/Diablo to be released from the mitochondrion to the cytosol, where these molecules trigger activation of caspases and eventually causes cell death. Among the various caspases, caspase-3 is considered as cell death executioner. It causes nuclear DNA cleavage by either directly translocating to the nucleus or by activation of caspase-dependent DNase [33-35]. In this study we observed increased number of caspase-3 positive neurons after AgNP incubation, suggesting activation of mitochondria-initiated, caspase-dependent cell death pathway by the AgNP. Selenium intervention reduced the number of caspase-3 positive cells, suggesting that selenium is capable of blocking caspase-dependent cell death pathway.

Conclusions

Silver nanoparticles induce cell toxicity through enhancing ROS production, causing mitochondrial membrane depolarization and activating caspase-3 dependent cell death pathway. Selenium protects cells from silver nanoparticle toxicity by reducing ROS production, holding up the mitochondrial membrane potential, and preventing caspase-3 activation.

Acknowledgements

LJ was supported by National Science Foundation of China (81260184) and Ningxia Medical University Research Fund (2010); PAL by the National Institute of Health (7R01DK075476-06). JJB and AV by NSF-BIO (DBI # 1044642) and NSF/EPA (Center for Environmental Implications of Nanotechnology (CEINT) and partially by NSF-PIRE (Award#1243433). (ZW by National Science Foundation of China (81060242). The BRITE is partially funded by the Golden Leaf Foundation.

Authors Contributions

Conceived and designed the experiments: PAL, JJB. Performed the experiments: WM, LJ, AV, SLM, ZW; Contributed reagents/materials/analysis tools: PAL, JJB. Wrote the paper: WM, PAL, JJB.

Competing Interests

The authors have declared that no competing interest exists.

References

1. Fordhamb WR, Redmond S, Westerland A, Cortes EG, Walker C, Gallagher C, Medina CJ, Waechter F, Lunck C, Ostrume RF, Caputo GA, Hettiger JD,

- Krchnavek RR. Silver as a Bactericidal Coating for Biomedical Implants. *Surface & Coatings Technology*. 2014; 253: 52-57.
2. Johnson AC, Jurgens MD, Lawlor AJ, Cisowska J, Williams RJ. Particulate and colloidal silver in sewage effluent and sludge discharged from British wastewater treatment plants. *Chemosphere*. 2014; 112: 49-55.
3. Ocwieja M, Adamczyk Z, Morga M, Kubiak K. Silver particle monolayers-Formation, stability, applications. *Adv Colloid Interface Sci*. 2014; DOI 10.1016/j.cis.2014.07.001
4. Key CS, Reaves D, Turner F, Bang JJ. Impacts of Silver nanoparticle ingestion on pigmentation and developmental progression in drosophila. *Atlas J Biol*. 2011; 1(3): 52-61.
5. Gao J, Sepúlveda MS, Klinkhamer C, Wei A, Gao Y, Mahapatra CT. Nanosilver-coated socks and their toxicity to zebrafish (*Danio rerio*). *Embryos. Chemosphere*. 2015; 119: 948-952.
6. Ahamed M, AlSalhi MS, Siddiqui MK. Silver nanoparticle applications and human health. *Clinica Chimica Acta*. 2010; 411:1841-1848.
7. Slawson RM, Lee H, Trevors JT. Bacterial interactions with silver. *Biomaterials*. 1999; 3(3-4): 151-154.
8. Chairuangkitti P, Lawanprasert S, Roytrakul S, Aueviriyavit S, Phummiratch D, Kulthong K, Chanvorachote P, Maniratanachote R. Silver nanoparticles induce toxicity in A549 cells via ROS-dependent and ROS-independent pathways. *Toxicol In Vitro*. 2013; 27:330-338.
9. Teodoro J, Simoes A, Duarte F, Rolo A, Murdoch R, Hussain S, Palmeira C. Assessment of the toxicity of silver nanoparticles in vitro: A mitochondrial perspective. *Toxicol In Vitro*. 2011; 23: 664-670.
10. Ribeiro F, Gallego-Urrea JA, Jurkschat K, Crossley A, Hassellöv M, Taylor C, Soares AM, Loureiro S. Silver nanoparticles and silver nitrate induce high toxicity to *Pseudokirchneriella subcapitata*, *Daphnia magna* and *Danio rerio*. *Sci Total Environment*. 2014; 466-467: 232-241.
11. Arai Y, Miyayama T, Hirano S. Difference in the toxicity mechanism between ion and nanoparticle forms of silver in the mouse lung and in macrophages. *Toxicology*. 2015; 328: 84-92.
12. Foldbjerg R, Olesen P, Hougaard M, Dang DA, Joffmann HJ, Autrup H. PVP-coated silver nanoparticles and silver ions induce reactive oxygen species, apoptosis and necrosis in THP-1 monocytes. *Toxicol Lett*. 2009; 190: 156-162.
13. Kemoto T, Kunito T, Tanaka H, Baba N, Miyazaki N, Tanabe S. Detoxification mechanism of heavy metals in marine mammals and seabirds: interaction of selenium with mercury, silver, copper, zinc, and cadmium in liver. *Arch Environ Contam Toxicol*. 2004; 47(3): 402-413.
14. Rayman MP. The importance of selenium to human health. *Lancet*. 2000; 356: 233-241.
15. Pillai R, Uyehara-Loch JH, Bellinger FP. Selenium and selenoprotein function in brain disorders. *IUBMB Life*. 2014; 66(4): 229-39.
16. Look MP, Rockstroh JK, Rao GS, Kreuzer KA, Barton S, Lemoch H, Sudhop T, Hoch J, Stockinger K, Spengler U, Sauerbruch T. Serum selenium, plasma glutathione (GSH) and erythrocyte glutathione peroxidase (GSH-Px)-levels in asymptomatic versus symptomatic human immunodeficiency virus-1 (HIV-1)-infection. *Eur J Clin Nutr*. 1997; 51: 266-272.
17. Ansari MA, Ahmad AS, Ahmad M, Salim S, Yousuf S, Ishrat T, Islam F. Selenium protects cerebral ischemia in rat brain mitochondria. *Biol Trace Elem Res*. 2004; 101:73-86.
18. Kiremidjian-Schumacher L, Roy M. Effect of selenium on the immunocompetence of patients with head and neck cancer and on adoptive immunotherapy of early and established lesions. *Biofactors*. 2001; 14: 161-168.
19. Zafar KS, Siddiqui A, Sayeed I, Ahmad M, Salim S, Islam F. Dose-dependent protective effect of selenium in rat model of Parkinson's disease: neurobehavioral and neurochemical evidences. *J Neurochem*. 2003; 84: 438-446.
20. Islam F, Zia S, Sayeed I, Zafar KS, Ahmad AS. Selenium-induced alteration of lipids, lipid peroxidation, and thiol group in circadian rhythm centers of rat. *Biol Trace Elem Res*. 2002; 90: 203-214.
21. Venardos K, Harrison G, Headrick J, Perkins A. Effects of dietary selenium on glutathione peroxidase and thioredoxin reductase activity and recovery from cardiac ischemia-reperfusion. *J Trace Elem Med Biol*. 2004; 18: 81-88.
22. Panee J, Liu W, Nakamura K, Berry MJ. The responses of HT22 cells to the blockade of mitochondrial complexes and potential protective effect of selenium supplementation. *Int J Biol Sci*. 2007; 3: 335-341.
23. Srivastava M, Singh S, Self WT. Exposure to silver nanoparticles inhibits selenoprotein synthesis and the activity of thioredoxin reductase. *Environ Health Perspect*. 2012; 120(1): 56-61.
24. Bang J, Yeyeodu S, Gilyazova N, Witherspoon S, & Ibeanu G. Effects of carbon nanotubes on a neuronal cell model in vitro. *Atlas J Biol*. 2011; 1(3): 70-77.
25. Kumari S, Mehta SL, Li PA. Glutamate induces mitochondrial dynamic imbalance and autophagy activation: preventive effects of selenium. *PLoS One*. 2012; 7:e39382.
26. Asharani PV, Hande MP, Valiyaveetil S. Anti-proliferative activity of silver nanoparticles. *BMC Cell Biol*. 2009; 10: 65.
27. Braydich-Stolle LK, Lucas B, Schrand A, Murdock RC, Lee T, Schlager JJ, Hussain SM, Hofmann MC. Silver nanoparticles disrupt GDNF/Fyn kinase signaling in spermatogonial stem cells. *Toxicol Sci*. 2010; 116(2): 577-589.
28. Kim S, Choi JE, Choi J, Chung KH, Park K, Yi J, Ryu DY. Oxidative stress-dependent toxicity of silver nanoparticles in human hepatoma cells. *Toxicol In Vitro*. 2009; 23(6): 1076-1084.
29. Oberdorster G, Elder A, Rinderknecht A. Nanoparticles and the brain: cause for concern? *J Nanosci Nanotechnol*. 2009; 9(8): 4996-5007.

30. Tiwari DK, Jin T, Behari J. Dose-dependent in-vivo toxicity assessment of silver nanoparticle in Wistar rats. *Toxicol Mech Methods*. 2011; 21(1): 13-24.
31. Govender R, Phulukdaree A, Gengan RM, Anand K, Chuturgoon AA. Silver nanoparticles of *Albizia adianthifolia*: the induction of apoptosis in human lung carcinoma cell line. *J Nanobiotechnology*. 2013; 11:5.
32. Hirsch T, Marzo I, Kroemer G. Role of the mitochondrial permeability transition pore in apoptosis. *Biosci. Rep.* 1997; 17(1): 67-76.
33. Kang M, Reynolds CP. Bcl-2 inhibitors: targeting mitochondrial apoptotic pathways in cancer therapy. *Clin Cancer Res*. 2009; 15: 1126-1132.
34. Kelly B, Salvesen G. Mechanisms of caspase activation. *Current Opinion Cell Biol*. 2003; 15:725-731.
35. Kasibhatla S, Tseng B. Why target apoptosis in cancer treatment? *Mol. Cancer Ther.* 2003; 2(6): 573-80.